Oct 19th, 12:00 AM

Elastic-plastic Interactive Buckling of Thin-walled Steel Compression Members

Dan Dubina

Viorel Ungureanu

Fifteenth International Specialty Conference on Cold-Formed Steel Structures
St. Louis, Missouri U.S.A., October 19-20, 2000

ELASTIC-PLASTIC INTERACTIVE BUCKLING OF THIN-WALLED STEEL COMPRESSION MEMBERS

Dan Dubina[1], Viorel Ungureanu[2]

[1] *Department of Steel Structures and Structural Mechanics, Civil Engineering and Architecture Faculty, The "Politehnica" University of Timisoara, Stadion 1, RO-1900, Timisoara, Romania*
[2] *Laboratory of Steel Structures, Centre of Advanced and Fundamental Technical Sciences, Romanian Academy of Sciences, Timisoara Branch, M. Viteazul 24, RO-1900, Timisoara, Romania*

KEYWORDS: Thin-walled cold-formed steel members, local buckling, local plastic mechanism, elastic overall buckling, imperfection, erosion, interactive plastic-elastic buckling.

ABSTRACT: In the actual design codes the interaction formula for local and overall buckling modes of thin-walled steel compression (TWSC) members, the effect of local buckling is introduced by means of effective strength of short members. This paper proposes to replace, into the Ayrton-Perry interaction formula, the short member "effective" strength, which is based on the "effective width" approach by the plastic strength evaluated by means of local plastic mechanism analysis. There are some papers by Murray et al. [1,2,3], in which the plastic mechanisms corresponding to the local buckling of plates and TWSC members in compression are analysed. On this basis, the local-overall interactive buckling modes can be regarded as interaction between local rigid-plastic mode and overall-elastic one, but until now it was difficult to couple these two modes into an adequate interactive equation. The paper shows the use of proposed "plastic-elastic" approach for the analysis of some series of plain and lipped channel specimens in compression. Comparisons with test and EUROCODE 3 results are presented.

INTRODUCTION

In case of TWSC members multiple local buckling modes may occur simultaneously under the same critical load. For a long member, multiple load buckling modes with ***m-1***, ***m***, ***m+1*** half-wave-length may interact in a first form of interaction (Fig. 1) and give rise to an unstable post-critical behaviour. It is very important to know that such interaction provides a ***localisation of the buckling*** patterns, because the localised mode has a more pronounced unstable slop than that periodical one. The second interaction is due to the interaction of the stable post-critical overall buckling with an unstable post-critical localised buckling and yields to a very unstable post-critical behaviour. This interaction produces a great erosion of the critical load due to geometrical imperfection, and characterises the behaviour of thin-walled members [4].

If the localised mode occurs prior to the overall one, the member post-buckling behaviour may be modified by material yielding and leads to a local plastic mechanism (Fig. 2). In this case, the interaction occurs between the overall mode, which corresponds to an elastic non-linear behaviour of the TWSC member, and the local plastic buckling of the component walls. Murray [1,2,3] has given a theoretical model of this type of behaviour, and provided a method, which closely predicts the localised large plastic displacement failure of thin-walled members. The problem is to identify correctly the plastic mechanism, because a quite confusing variety of such mechanisms exist.

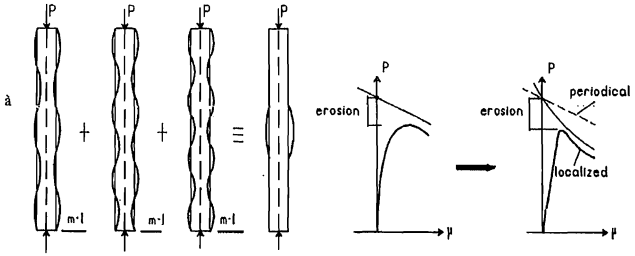

Fig. 1 –Localised buckling pattern generated by multiple local buckling modes interaction

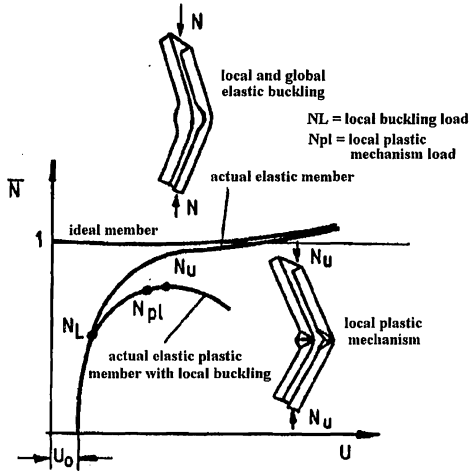

Fig. 2 – Thin-walled compression member behaviour

If the plastic mechanism is properly identified, the resistance of the short member, either in compression or bending, can be more appropriately evaluated, than using the "effective width" approach. The reason is that even local buckling firstly appears in case of short members, it always changes into local plastic mechanism when the member fails.

For stub columns the *"effective width"* approach operates with the plastic strength of the effective cross-section, while effective width of component walls is evaluated in terms of the elastic critical stress; this represents an important inconsistency of this theoretical model. The *"local plastic mechanism"* operates with the *"real"* plastic strength, assuming the TWSC stub column fails by forming plastic hinge and/or plastic zone, as effect of the localisation of buckling pattern. Consequently, the local-global interactive buckling is of *plastic-elastic* type, not an *elastic-elastic* one.

2. PLASTIC RESISTANCE OF THIN-WALLED STUB COLUMN

2.1 Local plastic mechanisms of thin-walled stub column

In order to investigate the plastic collapse of stub channel columns, Murray & Khoo [1] tested many channels with different cross-sections and observed five different plastic mechanisms (Fig. 3).

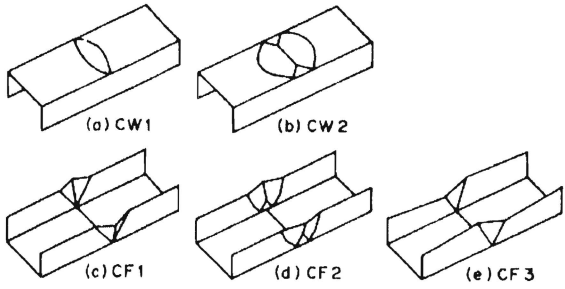

Fig. 3 – Five plastic mechanisms observed in laboratory tests on channel columns [1]

Figure 4 shows some examples of plastic mechanisms observed during the tests on plain and lipped channel stub columns, carried out in MSM Laboratory of the University of Liege [5,6].

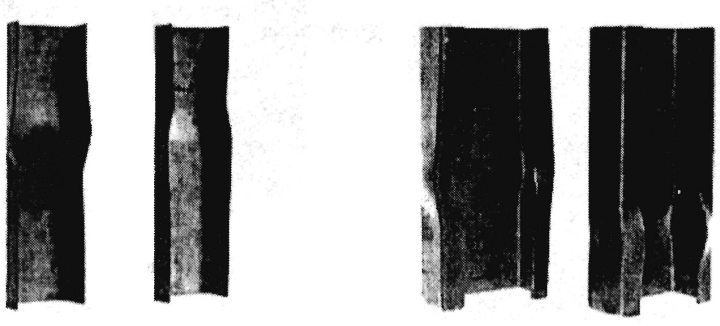

a) b)

Fig. 4 – Plastic mechanisms of plain and lipped channel stub columns

There are two major classes of plastic mechanisms i.e. *true mechanism* and *quasi-mechanism*. A true mechanism is one, which is developed from the original thin-walled member by folding the individual plates along the plastic hinge lines. A quasi-mechanism is one in which some regions of the individual plates of the structure are deformed by yielding in order to allow for plastified zones to deflect.

Murray & Khoo [1] and Mahendran & Murray [2], respectively, proposed some simple basic mechanisms (Fig. 5) which can be combined to draw up the more complicated ones obtained in practice.

The present study is focussed on the behaviour of plain and lipped channel sections. Table 1 gives the load-deflection formulae (N-Δ) for the four true plastic mechanisms used in this paper.

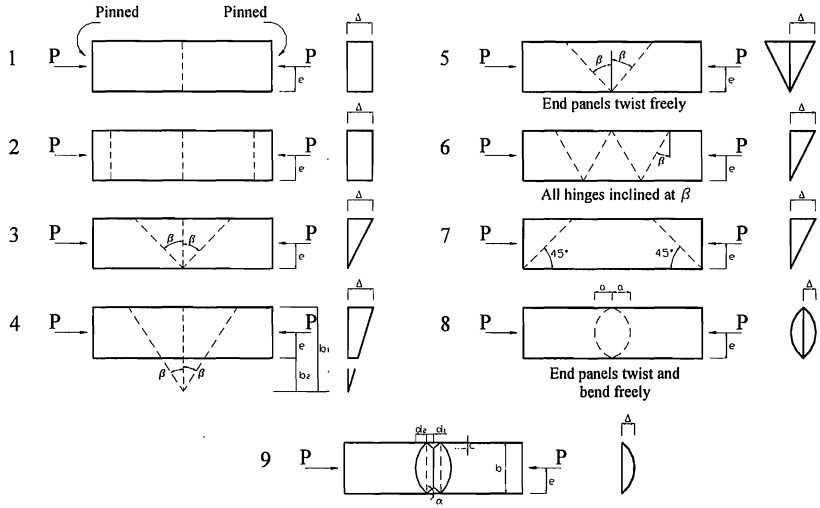

Fig. 5 –Basic plastic true mechanisms of thin-walled steel structures

Table 1 – True basic mechanisms used in this paper

Type 1	$N = \sigma_y tb\left\{\left[\left(\frac{2\Delta}{t}\right)^2+1\right]^{0.5}-\frac{2\Delta}{t}\right\}$; e=b/2
Type 3	$N=\frac{\sigma_y tb}{2}\left\{\left[\left(\frac{2\Delta}{\kappa_1 t}\right)^2+1\right]^{0.5}-\frac{2\Delta}{\kappa_1 t}+\frac{\kappa_1 t}{2\Delta}\ln\left\{\left[\left(\frac{2\Delta}{\kappa_1 t}\right)^2+1\right]^{0.5}-\frac{2\Delta}{\kappa_1 t}\right\}\right\}$ $Ne=\frac{\sigma_y t^3 b^2 \kappa_1}{12\Delta^2}\left\{\left[\left(\frac{2\Delta}{\kappa_1 t}\right)^2+1\right]^{3/2}-1-\left(\frac{2\Delta}{\kappa_1 t}\right)^3\right\}$; $\kappa_1 = 1+\sec^2\beta$
Type 8 Flip-disk mechanism	$N=\frac{\sigma_y tb}{6}\left\{1-\frac{2\Delta}{t}+\left[\left(\frac{2\Delta}{t}\right)^2+1\right]^{0.5}-\frac{6\Delta}{t\left(1+4a^2/b^2\right)}+4\sqrt{\left[\frac{3\Delta}{2t\left(1+4a^2/b^2\right)}\right]^2+1}\right\}$ e=b/2; a = 0.2×b
Type 9 Roof-shaped mechanism	$N=\sigma_y tb\left\langle\frac{b-2c}{b}\left\{\left[(1+r)^2\left(\frac{\Delta}{t}\right)^2+1\right]^{0.5}-(1+r)\left(\frac{\Delta}{t}\right)\right\}\right.$ $\left.+\frac{c}{b}\left\{\left[\Delta_{kt}^2+1\right]^{0.5}-\Delta_{kt}+\frac{1}{\Delta_{kt}}\ln\left(\Delta_{kt}+\left[\Delta_{kt}^2+1\right]^{0.5}\right)\right\}\right\rangle$ $\Delta_{kt}=\frac{2(1+r)}{k}\frac{\Delta}{t}$; $k=\cos ec^2(\alpha)+\cos ec^2(\beta)$; e=b/2; c = 0.2×b; r = 0.6

where:

Δ = lateral deflection of flange / web;

t = thickness of wall;

b = width of flange / web.

The mechanism type depends on the yielding strength of steel, slenderness ratio, b/t, and the level of initial geometrical imperfections of the TWSC member.

In Table 2 [2] is shown the influence of initial out-of-plane deflections, y_o and slenderness ratio b/t for plates subjected to in plane compression. It was observed that plates with large b/t ratio developed flip-disk mechanisms, while plates having smaller b/t ratio developed roof-shaped mechanisms.

Table 2 – Local plastic mechanisms for a yield stress of 250N/mm^2

b/t y_0/t	20	40	60	80	90	95	100
0.00	Roof	Roof	Roof	Roof	Roof	Roof	Flip-disk
0.03	Roof	Roof	Roof	Roof	Roof	Roof	Flip-disk
0.05	Roof	Roof	Roof	Roof	Roof	Flip-disk	Flip-disk
0.10	Roof	Roof	Roof	Roof	Roof	Flip-disk	Flip-disk
0.20	Roof	Roof	Roof	Roof	Flip-disk	Flip-disk	Flip-disk
0.30	Roof	Roof	Roof	Roof	Flip-disk	Flip-disk	Flip-disk
0.40	Roof	Roof	Roof	Flip-disk	Flip-disk	Flip-disk	Flip-disk
0.50	Roof	Roof	Flip-disk	Flip-disk	Flip-disk	Flip-disk	Flip-disk
0.60	Roof	Roof	Flip-disk	Flip-disk	Flip-disk	Flip-disk	Flip-disk
0.70	Flip-disk	Flip-disk	Flip-disk	Flip-disk	Flip-disk	Flip-disk	Flip-disk
1.00	Flip-disk	Flip-disk	Flip-disk	Flip-disk	Flip-disk	Flip-disk	Flip-disk

Rondal [7] analysed the influence of yield strength change and the effect of residual stresses on the behaviour of thin-walled cold-formed steel columns. Figure 6 shows the change of yield stress for plain channel and hat section specimens. Both the change of yield strength on the member cross-section and residual stresses are due to cold-forming and represents a characteristic of the cold-formed steel sections.

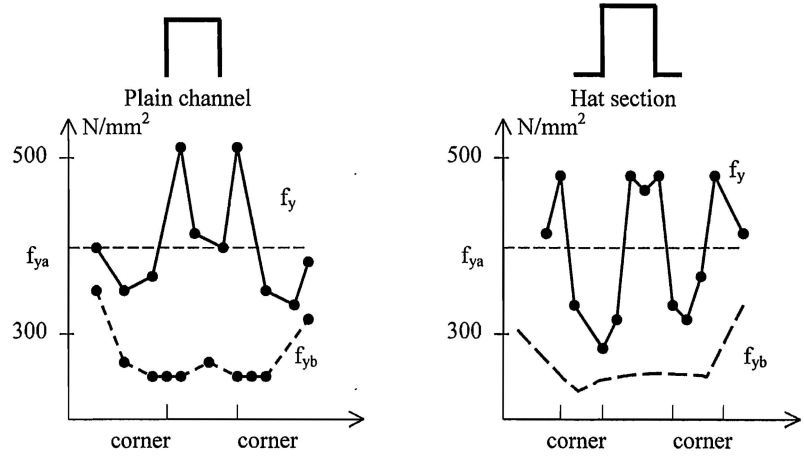

Fig. 6 – The influence of cold-forming process

Eurocode 3 Part 1.3 [8] provides a formula to evaluate the average design strength, f_{ya}, to take into account the influence of cold forming. This is:

$$f_{ya} = f_{yb} + (CNt^2/A_g) \times (f_u - f_{yb}) \quad (1)$$

where:

f_{yb} , f_u = characteristic tensile yielding strength and tensile ultimate strength of the basic material (N/mm^2);

t = material thickness before cold forming (mm);
A_g = gross cross sectional area (mm^2);
C = coefficient as a function of the type of forming;
C=7 for rolled material
C=5 for other methods of forming.
N = number of 90° bends in the section with an internal radius < 5t.

Starting from tests performed by Batista at the University of Liege on plain and lipped channels in compression [6], Table 3 shows the average design strength values, f_{ya}, compared with the yielding strength of the basic material, f_{yb}. It is easy to observe that f_{ya} is (5-10)% higher than f_{yb}.

Table 3 - Average design strength f_{ya} (N/mm^2)

Profile	Section $w_1 \times w_2 \times w_3 \times t$	r (mm)	f_{yb}	f_u	f_{ya}
U22	112×56×2	2	397	540	410
U33	75×60×2	2	397	540	412
U40	51×51×2	2	397	540	417
C10	103×36×21×2	2	397	468	425
C80	89×89×18×2	2	397	468	417
C86	100×100×20×1.5	1.5	376	468	384

In what concerns the residual stresses, Batista found for his tested plain channels that they do not exceed 40 N/mm^2, while for lipped channels they do not exceed 90 N/mm^2. Figure 7 presents the measured residual stresses for plain and lipped channel specimens. It can be seen that the average residual stresses are going in negative sense, both for flanges and webs, and compared with the change of yield strength, due to the cold forming, they are opposite.

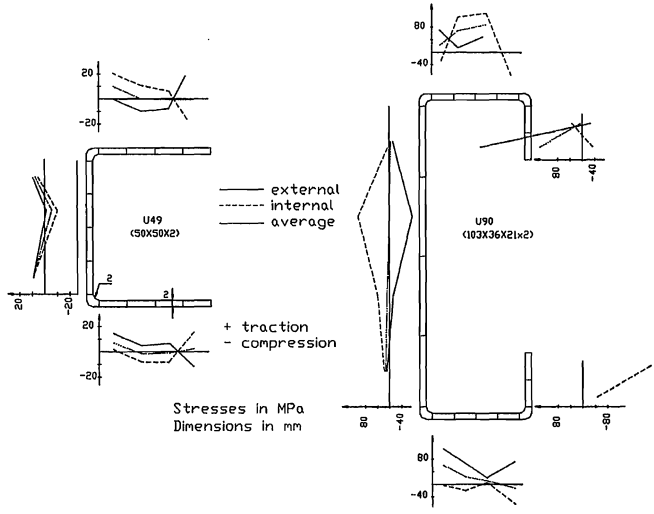

Fig. 7 - Measured residual stresses for plain channel and lipped channel specimens tested by Batista [6]

2.2 Numerical study of the ultimate strength of cold-formed stub columns. Comparison with experimental data

In this paragraph, the experimental data carried out in MSM Laboratory of the University of Liege [6] are compared with theoretical results obtained by rigid-plastic analysis. In Table 4 the main data dimensions for both plain and lipped channel specimens are shown.

Table 4 – Main data for plain and lipped channel specimens tested in Liege

Plain channel							
Profil	f_{ya} (N/mm^2)	f_{yb} (N/mm^2)	f_{yd} (N/mm^2)	h (mm)	b (mm)	t (mm)	L (mm)
U22	410	397	370	113	55	2.05	298
U33	412	397	372	76	60	2.06	399
U44	413	397	373	64	62	2.05	413
U18	413	397	373	94	47	2.04	250
U29	415	397	375	63	51	2.08	240
U40	417	397	377	51	51	2.04	224

Lipped channel								
Profile	f_{yb} (N/mm^2)	f_{ya} (N/mm2)	f_{yd} (N/mm^2)	h (mm)	b (mm)	c (mm)	t (mm)	L (mm)
C8	397	428	338	103	36	10	2.02	225
C10-1	397	425	335	106	35	21	2.03	241
C10-2	397	425	335	106	35	21	2.03	241
C10-3	397	425	335	106	35	21	2.03	242
C49	397	419	319	103	50	31	2.01	246
C78	397	418	318	89	89	10	2.07	355
C80-1	397	417	317	91	88	18	2.04	354
C80-2	397	417	317	91	88	18	2.04	354
C80-3	397	417	317	91	88	18	2.04	354
C82	397	416	316	91	89	27	2.07	353
C34	376	385	295	156	54	30	1.49	352
C84B	376	385	295	98	99	12	1.48	343
C86B-3	376	384	294	100	100	20	1.49	299
C86B-4	376	384	294	100	100	20	1.49	397

In Table 4, the geometry notations are the usual ones, while f_{yd} notation is the corrected value of average yield strength, in order to account for residual stresses.

The main aim of this study is to evaluate the reduction factor of plastic strength, Q_{pl}, of the thin-walled sections in compression. The following formula can be used:

$$Q_{pl} = \frac{N_{pl,m}}{A \cdot f_y}, \tag{2}$$

where $N_{pl,m}$ is the total plastic force corresponding to the forming of the local plastic mechanism. In fact, Q_{pl} represents the dimensionless ultimate plastic strength of a thin-walled stub column.

In case of plain channels, the quasi-mechanism corresponding to type 1 and type 3 true mechanisms was used. This quasi-mechanism is similar to local plastic mechanisms obtained in laboratory (see Fig. 4a). For this type of quasi-mechanism (see Fig. 8), Murray obtained the next formula:

$$N_{pl,m} = \frac{1}{2\overline{A}^2\overline{C}}\left[\delta + e - \overline{A}\overline{D} - \overline{B} - \left\{\left(\delta + e - \overline{A}\overline{D} - \overline{B}\right)^2 - 4\overline{A}^2\overline{C}\left(\overline{C}\overline{B}^2 + \overline{B}\overline{D} + \overline{F}\right)\right\}^{1/2}\right] \quad (3)$$

where:

$$\overline{A} = -\frac{1}{2f_y h}\ ;\ \overline{B} = \frac{t}{2} + \frac{P}{f_y h}\ ;\ \overline{C} = -f_y h\ ;\ \overline{D} = 2f_y th\ ;\ \overline{F} = 2P_f e_f - f_y h t^2/2$$

δ = member out of plane deflection, $\delta = \Delta^2 L/(2b^2 \tan\beta)$;
e = position of applied force P;
$f_{y,d}$ = corrected average yield strength with residual stresses;
L = length of the element.

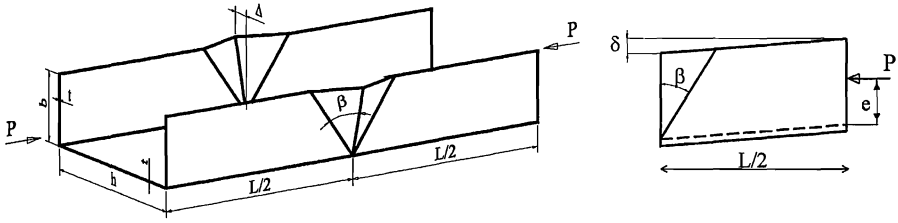

Fig. 8 – Model of local plastic mechanism of a plain channel column with flange failure

In case of lipped channel sections, the combined true mechanisms corresponding to roof-shaped mechanism for web and flange, and type 3 for lips were used, as shown in Figure 9. This combined mechanism is similar to the local plastic mechanism obtained in laboratory (see Fig. 4b). The total plastic force, $N_{pl,m}$ was obtained by simple addition of the values corresponding to the individual mechanisms.

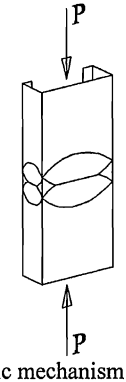

Fig. 9 – Model of the local plastic mechanism in case of lipped channel column

The results corresponding to stub column specimens tested in Liege are shown in Table 5. The following notations were used: Q_{EC3}, is the reduction coefficient for effective area calculated with EUROCODE 3 Part. 1.3 formulae, which, in fact, is equal with the dimensionless value of stub column ultimate strength, Q_{exp}, is the dimensionless experimental ultimate strength of stub column, e.g.

$$Q_{EC3} = \frac{A_{eff} \cdot \sigma_{max}}{A \cdot f_y} = \frac{A_{eff}}{A};\ \sigma_{max} = f_y\ ; \quad (4)$$

$$Q_{exp} = \frac{N_{u,exp}}{A \cdot f_y} \quad (5)$$

It can be seen from Table 5 that compared with Q_{EC3}, the plastic reduction factor Q_{pl} is in a better agreement with experimental values, Q_{exp}.

Table 5

Plain channel section			
Profile	Q_{pl}	Q_{EC3}	Q_{exp}
U22 Q	6.5 7	6.5	6.581
U33	6. 46	6. 69	6. 9
U44	6. 26	6. 16	6. 23
U18	6. 43	6. 45	6. 4
U29	6.712	6. 91	6.734
U46	6.767	6. 4	6.735
m	6. 48	6. 31	6. 5
s	6.655	6.645	6.6 1
m-1. 4s	6.558	6.557	6.5 4

Lipped channel section			
Profil	$Q_{plastic}$	$Q_{eff,EC3}$	Q_{exp}
C8	6. 81	6.776	6.712
C16-1	6.751	6.865	6.774
C16-2	6.751	6.865	6.7 3
C16-3	6.751	6.865	6.779
C49	6. 7	6.7 8	6.762
C78	6.5 4	6.438	6.5 8
C86-1	6.722	6. 42	6.738
C86-2	6.722	6. 42	6.756
C86-3	6.722	6. 42	6.718
C82	6. 96	6.769	6.761
m	6.762	6.763	6.726
s	6.657	6.11	6.6 1
m-1. 4s	6. 68	6.512	6. 21
C34	6.584	6.582	6.593
C84B	6.443	6.368	6.447
C8 B-3	6.513	6.4 5	6.528
C8 B-4	6.513	6.4 5	6.562
m	6.513	6.455	6.518
s	6.657	6.112	6.6 6
m-1. 4s	6.419	6.271	6.419

3. THE INTERACTIVE ELASTO-PLASTIC BUCKLING OF COLD-FORMED THIN-WALLED STEEL MEMBERS

3.1 The ECBL approach for interactive buckling

The ECBL approach [9] gives the possibility to couple the rigid-plastic local mode with the elastic overall one. The main problem of this approach is to evaluate properly the erosion of critical load into the *"interactive slenderness range"*. However, the evaluation of erosion is possible using some relevant experimental values [16] or numerical simulations [11].

The plastic reduction factor Q_{pl} of TWSC members can be obtained following the method presented in previous paragraph. According with ECBL approach, in case of a TWSC member, the two theoretical simple instability modes in interaction are the Euler mode, $\overline{N}_E = 1/\overline{\lambda}^2$ and the local one, here represented by $\overline{N}_{U,L} = Q_{pl}$. The resulting eroded curve, which describes the coupled instability mode, is $\overline{N}(\overline{\lambda}, Q_{pl}, \psi)$ (see Figure 10).

Theoretically, the maximum erosion of critical load, due both to the imperfections and coupling effect, occurs in the interaction point M $(\overline{\lambda} = 1/\sqrt{Q_{pl}})$, and the erosion factor ψ is defined as:

$$\psi = \overline{N}_E(\overline{\lambda}_C) - \overline{N}(\overline{\lambda}_C, \psi, Q_{pl}) = \overline{N}_{U,L} - \overline{N}(\overline{\lambda}_C) \tag{6}$$

where:

N_U = ultimate compression resistance of TWSC members;
N_{pl} = $A \times f_y$ full plastic resistance of TWSC members;
A = the gross area of cross section;
$\overline{N}_{U,L} = Q_{pl}$, plastic buckling resistance of short TWSC members (rigid plastic mode);
$\overline{\lambda}$ = relative slenderness in overall buckling;
$\overline{\lambda}_{U,L}$ = relative slenderness of short TWSC members ($\overline{\lambda}_{U,L} = 0.2$, for compression members);
$\overline{\lambda}_C$ = relative slenderness in the coupling point.

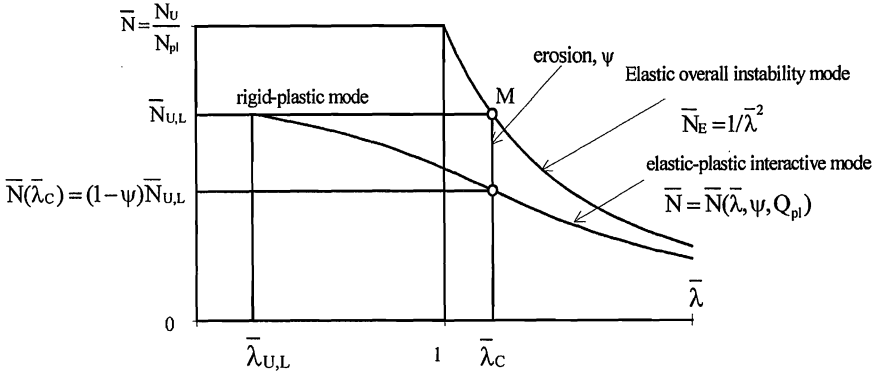

Fig. 10- The Interactive Buckling Model based on the ECBL Theory

The Ayrton-Perry equation is used to plot European buckling curves for hot-rolled members [13]. The solution of this equation may be easily adapted for thin-walled cold-formed members in compression [9], but this time Q_{EC3} will be replaced with Q_{pl}. From Figure 10 results:

$$\overline{N} = \frac{1 + \alpha(\overline{\lambda} - 0.2) + Q_{pl}\overline{\lambda}^2}{2\overline{\lambda}^2} - \frac{1}{2\overline{\lambda}^2}\sqrt{[1 + \alpha(\overline{\lambda} - 0.2) + Q_{pl}\overline{\lambda}^2]^2 - 4Q_{pl}\overline{\lambda}^2} = (1-\psi)Q_{pl} \tag{7}$$

where:

$$\overline{\lambda} = 1/\sqrt{Q_{pl}} \tag{8}$$

From the upper formulas results:

$$\alpha = \frac{\psi^2}{1-\psi} \cdot \frac{\sqrt{Q_{pl}}}{1 - 0.2\sqrt{Q_{pl}}} \tag{9}$$

This represents the formula of "α" imperfection coefficient which should be introduced in European buckling curves in order to adapt these curves for plastic-elastic model of interactive buckling of thin-walled cold-formed members. The "α" imperfection factor should be calibrated in terms of ψ and Q_{pl} factors.

There are two practical ways that can be used to evaluate the ψ erosion factor:

1. the *experimental procedure* which involves a statistical analysis of a representative series of test results corresponding to specified cross-section shapes, characterised by means of Q_{pl} factor in the *slenderness range of interactive buckling*; i.e. $\bar{\lambda} = 1/\sqrt{Q_{pl}} \pm \varepsilon$ (see Fig. 11);

   Both, the "mean approach" [10] or the "Eurocode 3 Annexe Z approach" [12] can be used to evaluate experimentally the erosion factor ψ.
2. the *numerical approach* based on Finite Element (FEM) or Finite Strip (FSM) non-linear analysis of the behaviour of thin-walled columns in the vicinity of critical bifurcation point [11].

This paper use of the ECBL "mean" approach for the case of experimental procedure.

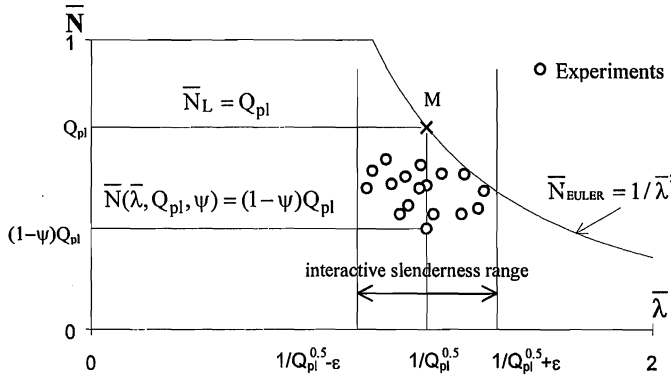

Fig. 11 - Evaluation of ψ Erosion Factor by means of experimental tests

3.2 Numerical results

The experimental data carried out at the University of Liege [6] were used to compare the ECBL plastic-elastic approach with the elastic-elastic one, and with EC3-Part. 1.3 results.

If the interactive slenderness range is assumed to be $\bar{\lambda} \pm \varepsilon = 1/Q_{pl}^{0.5} \pm 0.20$ [10], the experimental "mean" approach includes the following steps:

1. Compute the *individual* erosion for the ***i*** column specimen

$$\psi_i = Q_{pl} - N_{i,exp} \tag{10}$$

where

$$N_{i,exp} = \frac{N_{i,exp}}{N_{i,pl}} \tag{11}$$

with $N_{i,exp}$ - the experimental failure load and $N_{i,pl} = A_i \times f_y$ - the full plastic resistance of the ***i*** specimen.

2. Compute the mean value of ψ erosion factor for all ***n*** specimens with the same cross-section shape, included into the interactive slenderness range:

$$\psi_m = \frac{1}{n}\sum_{i=1}^{n}(Q_{pl} - N_{i,exp}) \tag{12}$$

3. Compute the *design* value of the erosion factor:

$$\psi_d = \psi_m + 1.64s \tag{13}$$

in which s is the standard deviation related to ψ_i and ψ_m values.

Figures 12 and 13 show the results for plain channels, while Figures 14 to 16 the results for lipped channels. According to Eurocode 3 Part. 1.3 the safety factor, γ_{M1}=1.1, was used for all numerical results.

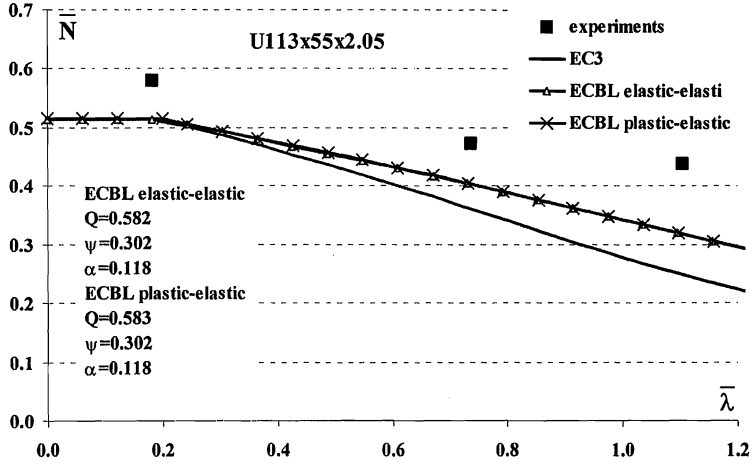

Fig. 12 - Numerical/Experimental Comparison for Plain Channel Sections subject to Compression tested by Batista [6]

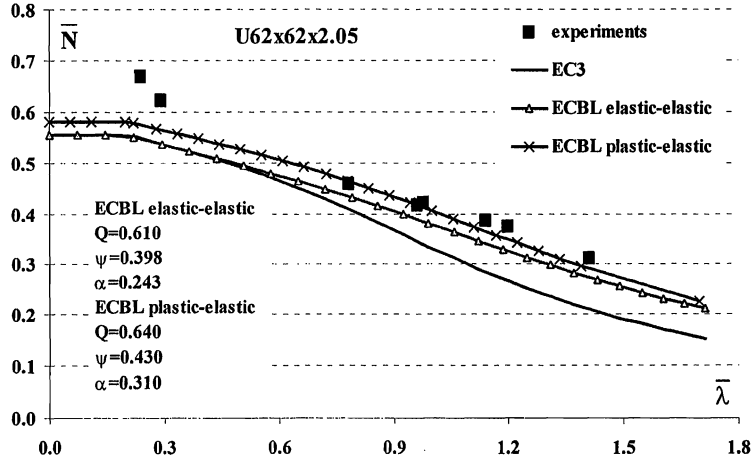

Fig. 13 - Numerical/Experimental Comparison for Plain Channel Sections subject to Compression tested by Batista [6]

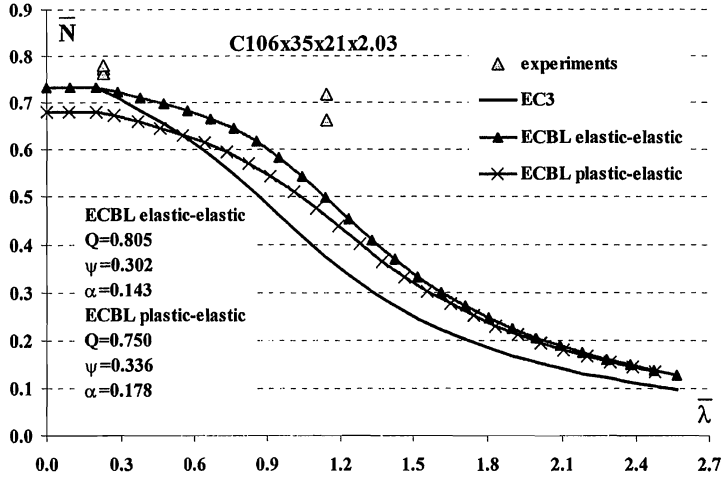

Fig. 14 - Numerical/Experimental Comparison for Lipped Channel Sections subject to Compression tested by Batista [6]

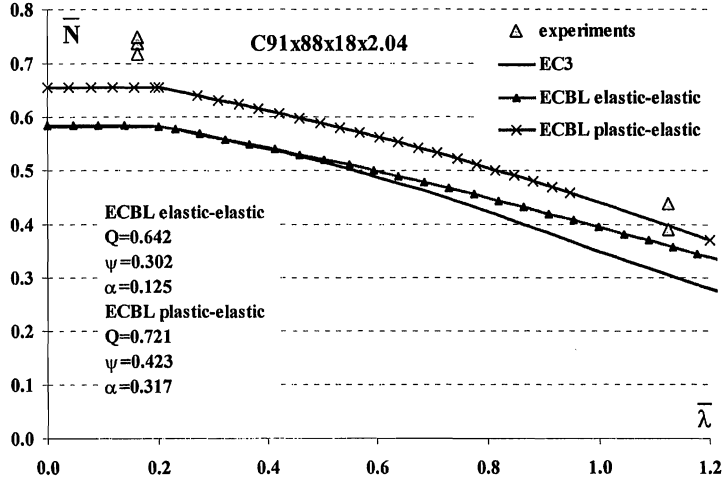

Fig. 15 - Numerical/Experimental Comparison for Lipped Channel Sections subject to Compression tested by Batista [6]

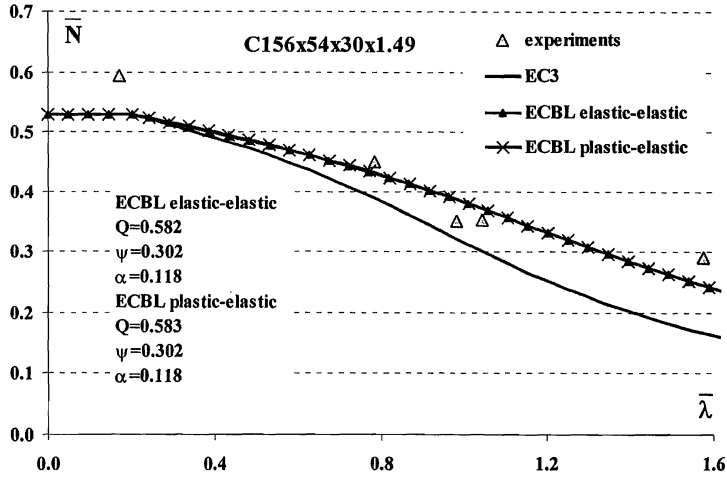

Fig. 16 - Numerical/Experimental Comparison for Lipped Channel Sections subject to Compression tested by Batista [6]

4. CONCLUSIONS

a) The local rigid-plastic model, proposed by Murray and developed in this paper describes properly the behaviour of thin-walled stub columns. This model is consistent with the real phenomenon of stub columns failure and is confirmed by test results. However, the crucial problem is the correct estimation of yield strength value accounting for the effects of cold forming. Even the present study was focussed on the behaviour of members in compression, the extension of propose model to the members in bending or in bending and compression can be done without major difficulties.

There is no distinction in this study between local and distortional instability modes. The first assumption of the local rigid mode was in correspondence with the local buckling of the thin-walled sections, but there is no problem to model the distortional mode too.

b) The ECBL approach was used to obtain a plastic-elastic interactive formula in a similar format as the actual buckling curves are expressed. Due to the lack of dedicated experimental values, the rigorous Eurocode 3 Annexe Z procedure [12] was not possible to be used for the erosion factor calibration. It is expected that with a dedicated experimental data base the use of Annex Z procedure will improve the results. However, the actual results are encouraging enough to continue this study.

c) The plastic-elastic interactive model naturally describes the phenomenon of the interactive buckling of thin-walled members, but further research is necessary in order to validate this approach.

5. REFERENCES

[1] N.W. Murray, P.S. Khoo: *Some basic plastic mechanisms in the local buckling of thin –walled steel structures*, Int. J. Mech. Sci., Vol. 23, No. 12, pp. 703-713, 1981.

[2] M. Mahendran, N.W. Murray: *Effect of initial imperfections on local plastic mechanisms in thin steel plates with in-plane compression*, Int. Conf. on Steel and Aluminium Structures – ICSAS 91, Singapore, 22-24 May 1991.

[3] N.W. Murray: *Introduction to the theory of thin-walled structures*, Oxford University Press, Oxford, 1984.
[4] D. Dubina: *Coupled instabilities in bar members – General Report*, CIMS'96-The Second Conference on Coupled Instabilities in Metal Structures, Liege, Belgium, September 5-7 1996, p. 119-132.
[5] E. Batista, C. Costa Ferreira & J. Rondal: *Stub-column strength of thin-walled profiles*, ECCS Colloquium on Stability of Plates and Shell Structures, Ghent, Belgium, April 6-8, 1987, pp. 219-224.
[6] E. Batista: *Essais de profils C et U en acier plies a froid. Universite de Liege, Laboratoire de Stabilite des Constructions*, Raport N° 157 157, 1986.
[7] J. Rondal: *Determination theoretique des contraintes residuelles dans les elements en acier profiles a froid*, Ce travail a recu le prix N.V. BEKAERT S.A. 1992, octroye par le Fonds National de la Recherche Scientifique.
[8] EUROCODE 3, Design of Steel Structures Part 1.3: *General rules. Supplementary rules for cold-formed thin gauge members and sheeting*, ENV 1993-1-3, February 1996.
[9] D. Dubina: *Coupled Instabilities in Thin-Walled Structures; Erosion Coefficient Approach in Overall-Local Buckling Interaction*, Research Report Ref. ERB 3510PL922443, Commission of the European Communities for Co-operation in Science and Technology with Central and Eastern European Countries, Liege, October 1993.
[10] D. Dubina, M. Georgescu, D. Goina, V. Ungureanu, E. Iorgovan: *Cold-Formed Steel Sections Experimental Data Base*, Thirteenth International Speciality Conference on Cold-formed Steel Structures, St. Louis, Missouri, USA, October 17-18, 1996, p. 665.
[11] D. Dubina, D. Goina, R. Zaharia, V. Ungureanu: *Numerical Modelling of Instability Phenomena of Thin-walled Steel Members*, The 5th International Colloquium on Stability and Ductility of Steel Structures, SDSS'97 (ed. T. Usami), Nagoya, Japan, 29-31 July 1997, vol. 2, p.755.
[12] M. Georgescu, D. Dubina: *E.C.B.L. and EUROCODE 3 Annex Z based calibration procedure for buckling curves of compression steel members*, 6th International Colloquium on Stability and Ductility of Steel Structures - SDSS'99, Timisoara, 9-11 September, 1999, p. 501.
[13] R. Maquoi, J. Rondal: *Mise en equation des nouvelles courbes europeennes de flambement.* Construction Metallique, N° 1, 1978.